J. Plasma Fusion Res. SERIES, Vol. 6 (2004) 156–159

Physical Properties of Plasma Ion Dynamics in Various Equilibria of Field-Reversed Configuration

TAKAHASHI Toshiki, UBUKATA Mieko, IWASAWA Naotaka[1] and KONDOH Yoshiomi

Gunma University, Kiryu 376-8515, Japan

[1]Satellite Venture Business Laboratory, Gunma University, Kiryu 376-8515, Japan

(Received: 9 December 2003 / Accepted: 28 January 2004)

Abstract

Single particle orbits are traced in the prescribed equilibria inside the separatrix of Field-Reversed Configurations (FRCs). Equilibria inside the separatrix with the peaked, flat and hollow current profile are calculated semi-analytically. The surface of section plot is used to visualize the regular and stochastic ion motion. In particular, stochasticity in a kinetic ion (i.e., the large gyro-radius ion) and magnetohydrodynamic (MHD) ion (i.e., the small gyro-radius ion) motion is studied; the majority of the kinetic ions are found to exhibit an adiabatic motion. It appears that the azimuthal drift velocity for the stochastic and kinetic ions in the elliptic FRC is larger than for the adiabatic ions because of a curvature drift in the neighborhood of the midplane. In the racetrack FRC, on the other hand, no significant difference is observed in the drift velocity in spite of the stochastic motion.

Keywords:

FRC, single particle motion, drift velocity, stochasticity, adiabaticity, equilibrium, current profile

1. Introduction

The tilt mode stability is the major physical issue of Field-Reversed Configurations (FRCs) [1-5]. Although the MHD predicts the FRC plasmas are unstable against the tilt mode [6,7], however, the several experimental measurements show their resilient feature [8]. Since the averaged beta value of FRC is near unity and thus an ion Larmor radius is comparable to the scale length, a fluid model approximation breaks and the velocity distributions become more important to expect an FRC's global behavior. In the FRCs, there are three types of particle trajectories depending on its velocity. A faster ion with large canonical angular momentum ($P_\theta \equiv mv_\theta r + q\psi(r, z)$, where m and q are the ion mass and charge, v_θ is the azimuthal velocity, ψ is the flux function, and r and z are the radial and axial position) exhibits betatron orbit encircling the geometric axis. A fast ion but with a smaller P_θ than the betatron particle draws a figure-8 orbit. The direction of its gyrating motion is changed due to the field reversal. These two peculiar trajectories may cause a kinetic stability of FRCs, and therefore the properties of ion dynamics should be investigated. On this viewpoint, Hayakawa *et al.* studied stochasticity or adiabaticity of ion motion in the deuterium-helium 3 fueled fusion plasma [9]. The existence of adiabatic and trapped particle in the curved magnetic line region was shown in [9], and it may cause a stabilizing flow to the tilt mode activity. However, only Hill's vortex model [10] was employed for the equilibrium of FRC, and how the equilibrium field affects the particle orbit is still unclear.

In the present study, the ion dynamics in the various equilibria of FRC inside the separatrix is studied.

2. Computational model

2.1 Equilibrium

The FRC equilibrium state is obtained by solving the Grad-Shafranov (G-S) equation for the flux function

$$r\frac{\partial}{\partial r}\left(\frac{1}{r}\frac{\partial \psi}{\partial r}\right)+\frac{\partial^2 \psi}{\partial z^2}=-\mu_0 r^2\frac{\mathrm{d}P}{\mathrm{d}\psi},$$

$$\frac{\mathrm{d}P}{\mathrm{d}\psi}=\frac{\Delta P}{\psi_{ax}}\left[\gamma+2(1-\gamma)\frac{\psi}{\psi_{ax}}\right], \qquad (1)$$

where ΔP is the pressure difference between the magnetic axis (i.e., the field-null O-point) and the separatrix and ψ_{ax} is the flux function at the magnetic axis. The parameter γ controls the current profile. Peaked current profiles are obtained for $0 \le \gamma < 1$, the flat one is for $\gamma = 1$, and the hollow current profiles are for $1 < \gamma \le 2$. The G-S equation is solved analytically and numerically using the method developed earlier [11,12]; the method is slightly modified here in order to obtain the peaked current profile. The normalized G-S equation becomes

Corresponding author's e-mail: t-tak@el.gunma-u.ac.jp

$$4\frac{\partial^2\psi}{\partial\rho^2}+\frac{1}{\rho}\frac{\partial^2\psi}{\partial z^2}=-\sigma\left[\frac{\gamma}{2}+(1-\gamma)\psi\right], \qquad (2)$$

where $\rho \equiv (r/r_s)^2$, $z/r_s \to z$, $\psi/\psi_{ax} \to \psi$, and $\psi_{ax} \equiv r_s^2 B_s/\sqrt{\sigma}$. The quantities r_s and B_s are the separatrix radius and the magnetic field at the separatrix and midplane, respectively. The parameter σ is obtained from the condition that the normalized flux function at the magnetic axis is unity. The solution to Eq. (2) is

$$\psi(\rho,z)=\sum_{n=0}^{N}C_n R^{(n)}(\rho)\cos\left[\left(n+\frac{1}{2}\right)\frac{\pi}{E}z\right]+A(\rho),$$

$$R^{(n)}(\rho)=\sum_{k=1}^{k_{max}}a_k\rho^k. \qquad (3)$$

The coefficients a_k are numerically calculated by solving the following recurrence formula:

$$(k+1)(k+2)a_{k+2}+\frac{\sigma(1-\gamma)}{4}a_k=\frac{\nu^2}{4}a_{k+1},$$

$$a_1=1,\ a_2=\frac{\nu^2}{8},\ \nu=\left(n+\frac{1}{2}\right)\frac{\pi}{E}, \qquad (4)$$

where E is the separatrix elongation. The function $A(\rho)$ is different with the current profile control parameter γ, and is written as follows:

$$A(\rho)=\frac{\gamma}{2(1-\gamma)}\left[\cos\left(\sqrt{\frac{\sigma(1-\gamma)}{4}}\rho\right)-1\right]$$

$0 \le \gamma < 1$ (for the peaked current profile),

$$A(\rho)=-\frac{\sigma}{16}\rho^2 \qquad \gamma = 1 \text{ (for the flat current profile)},$$

$$A(\rho)=\frac{\gamma}{2(1-\gamma)}\left[\cosh\left(\sqrt{\frac{\sigma(\gamma-1)}{4}}\rho\right)-1\right]$$

$1 < \gamma \le 2$ (for the hollow current profile).

Unknown expansion coefficients C_n are determined numerically by the boundary condition to set the flux function to be zero on the separatrix surface. The separatrix shape is given in the form [12],

$$\rho_s(z)=1-\left(\frac{z}{E}\right)^{2\mu}.$$

When μ = 1, the separatrix is in the elliptic shape. The racetrack separatrix is obtained for μ > 1. The obtained equilibrium states are shown in Fig. 1, where E = 5.0 for all the cases and μ = 4 for the racetrack separatrix and μ = 1 for the elliptic separatrix. The parameter γ is chosen as 0.5, 1.0 and 1.5 for peaked, flat and hollow current profile. The corresponding current profiles on the midplane (z = 0) are shown in Fig. 2. Since the contour lines for the hollow current profile are concentrated near the separatrix, therefore a steep density gradient is found to be located near the separatrix. On the other hand, uniform density is observed near the field-null O-point for the hollow current profile. On the contrary to the racetrack FRC, a curvature of the field line is found around the midplane in the elliptic case. The difference may affect the azimuthal drift velocity.

2.2 Calculation of ion orbit

Ion orbits in the prescribed equilibrium magnetic field are traced by solving the equation of motion

$$m\frac{\mathrm{d}\boldsymbol{v}}{\mathrm{d}t}=q(\boldsymbol{v}\times\boldsymbol{B}). \qquad (5)$$

The cylindrical coordinate system (r, θ, z) is used in the present study. The magnetic field in eq. (5) is calculated from the flux function

$$B_z=\frac{1}{r}\frac{\partial\psi}{\partial r},\ B_r=-\frac{1}{r}\frac{\partial\psi}{\partial z}. \qquad (6)$$

If the semi-analytical solution eq. (3) is directly used, the computation to trace the ion orbit needs a lot of time because of the summation with respect to k and n in eq. (3). Therefore, the flux function is calculated with the aid of eq. (3) only at the grid mesh points in the $r - z$ plane. The magnetic field at an ion's position is calculated by the interpolation method. To observe the ion motion, the surface of section plot is employed [9]. The surface intersecting the minimum B point along the line of forces is chosen as a plotting surface for the small-gyroradius and figure-8 particles, because due to the conservation of the magnetic moment, the force toward the

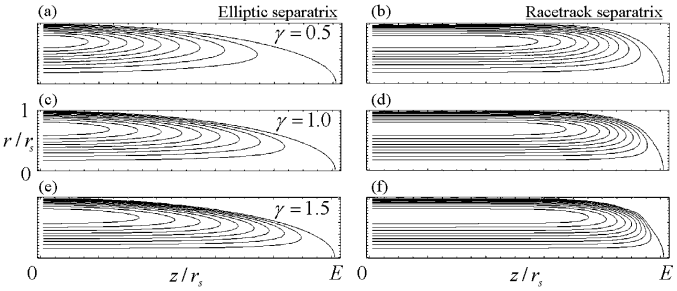

Fig. 1 Various equilibria inside the elliptic and racetrack separatrix (a) (c) (e). The elliptic separatrix shape (μ = 1) (b) (d) (f). The racetrack separatrix shape (μ = 4). Figures are shown for the (a) (b) peaked (γ = 0.5), (c) (d) flat (γ = 10), and (e) (f) hollow (γ = 0.5) current profile.

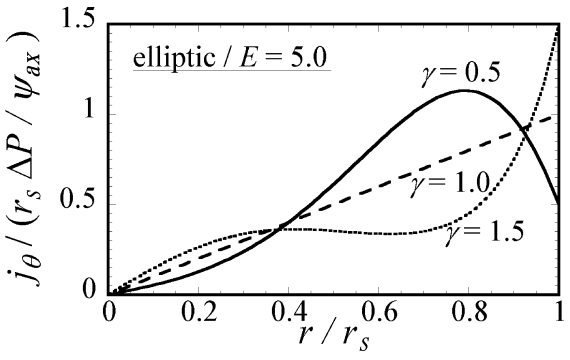

Fig. 2 The current profile on the midplane. The peaked (solid line), flat (dashed line), and hollow (dotted line) current profiles are shown.

minimum B point acts on all these ions. On the other hand, we can find the betatron particles that never cross the minimum B surface. Therefore, for the betatron particles, the following plotting surface is used, which satisfies,

$$\frac{\partial U}{\partial r}=0,\ U(r,\ z;\ P_\theta)\equiv\frac{\left(P_\theta-q\psi(r,\ z)\right)^2}{2mr^2}$$

where U is the effective potential known as the *Störmer potential* [13].

In a plasma without the electric field, the kinetic energy $K \equiv mv^2/2$ and the canonical angular momentum P_θ are constants of motion, and then these are good measures to characterize the ion motion. The new constants $\bar{s}$ and α instead of them are defined:

$$\bar{s}\equiv\int_R^{r_s}\frac{r}{r_s}\frac{\mathrm{d}r}{\rho_i},\ \rho_i=\frac{\sqrt{2mK}}{qB}$$

$$\alpha\equiv\frac{P_\theta}{q\psi(r=R,z=0)},$$

where R is the field-null circle radius. The constant $\bar{s}$ is a measure to discuss the finite Larmor radius (FLR) effect and α is a measure to give location of a guiding center and an orbit type (i.e., betatron etc.). Note that $\bar{s}$ is slight different from its definition customary used [1]; the Larmor radius in the customary definition is determined by the plasma temperature.

3. Results and discussion

All the calculation is done for the separatrix elongation E = 5. The current profile control parameter γ is 0.5 for the peaked profile, 1.0 for the flat and 1.5 for the hollow profile. The FLR parameter $\bar{s}$ is 2 for the kinetic case and 10 for the MHD case. The solution of the flux function to the G-S equation is applicable only inside the separatrix, and thus the particle orbit outside the separatrix is never traced. Our calculation therefore is restricted inside the separatrix.

The results from the surface of section plot are shown in Fig. 3. The kinetic ions (i.e., $\bar{s}$ = 2) tend to exhibit an adiabatic motion. On the other hand, the MHD ions (i.e., $\bar{s}$ = 10) are found to move stochastically. The orbit type of the MHD ion with large axial velocity is changed, when it passes through the curved magnetic line region. For instance, when a gyrating ion enters the region where the magnetic line is curved, its orbit is changed to the figure-8 or betatron. This is an origin of stochastization due to randomization of gyro-phase. On the contrary to the MHD ions, a kinetic ion encircles the geometric axis and exhibits a betatron motion; the type of orbit is never changed. Hence it moves adiabatically. There is no significant effect of the current profile on the behavior of ion motion as shown in Fig. 3. The percentages of adiabatic ions in the surface of section plot are summarized in Table 1. Although they show the number of test ions, however, it relates with the macroscopic number density. More adiabatic ions are found in the kinetic case ($\bar{s}$ = 2) than the MHD case ($\bar{s}$ = 10) for all the equilibria. The ions with larger canonical

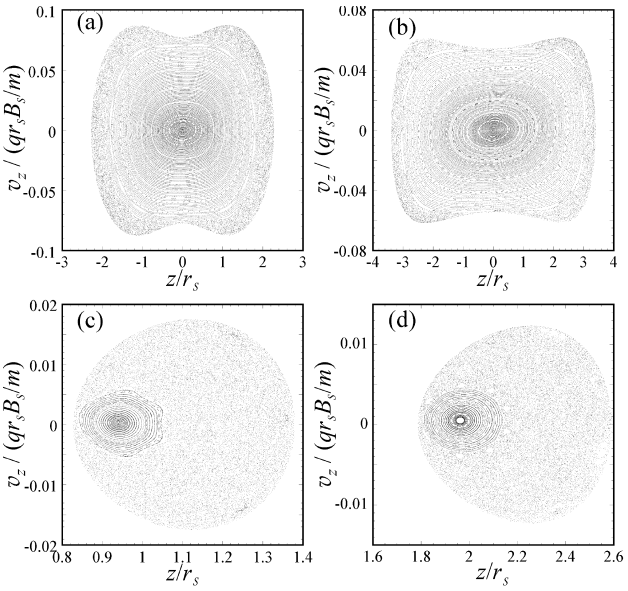

Fig. 3 The surface of section plots for ions with α = 0.8 in the elliptic FRC. (a) $\bar{s}$ = 2 (the kinetic case) and γ = 0.5 (the peaked current profile), (b) $\bar{s}$ = 2 and γ = 1.5 (the hollow current profile), (c) $\bar{s}$ = 10 (the MHD case) and γ = 0.5, and (d) $\bar{s}$ = 10 and γ = 1.5.

Table 1 The percentages of adiabatic particles

$\bar{s}$ = 2

	Elliptic separatrix			Racetrack separatrix		
α	Peaked	Flat	Hollow	Peaked	Flat	Hollow
0.7	75	79	83	92	94	93
0.8	83	88	90	95	96	95
1	100	100	100	100	100	100
1.2	100	100	100	100	100	100
1.4	100	100	100	100	100	100

$\bar{s}$ = 10

	Elliptic separatrix			Racetrack separatrix		
α	Peaked	Flat	Hollow	Peaked	Flat	Hollow
0.2	26	18	20	0	0	0
0.4	26	25	10	0	0	0
0.6	22	35	33	11	0	0
0.8	38	39	41	43	40	28
1.0	100	100	100	100	100	100

angular momentum (i.e., the ions with large α) are found to exhibit an adiabatic motion. They are confined only near the field-null O-point and have betatron orbits ($\alpha \geq 1$).

The azimuthal drift velocity of ions contributes to the global characteristic of FRC, and then its dependence on α(or P_θ) is shown in Fig. 4. There is no effective drifting motion in the MHD case, if they have a small gyro-radius or figure-8 orbit. A slight difference among equilibria can be seen; the drift velocity is the largest in the peaked current profile. In the kinetic case, even figure-8 and small-gyroradius ions (i.e., $\alpha < 1$) drift in the diamagnetic direction. Though stochasticity does not affect the drift motion in the MHD case, however, the stochastic fast ions in the elliptic FRC are found to have a larger drift velocity due to the curvature of the magnetic field.

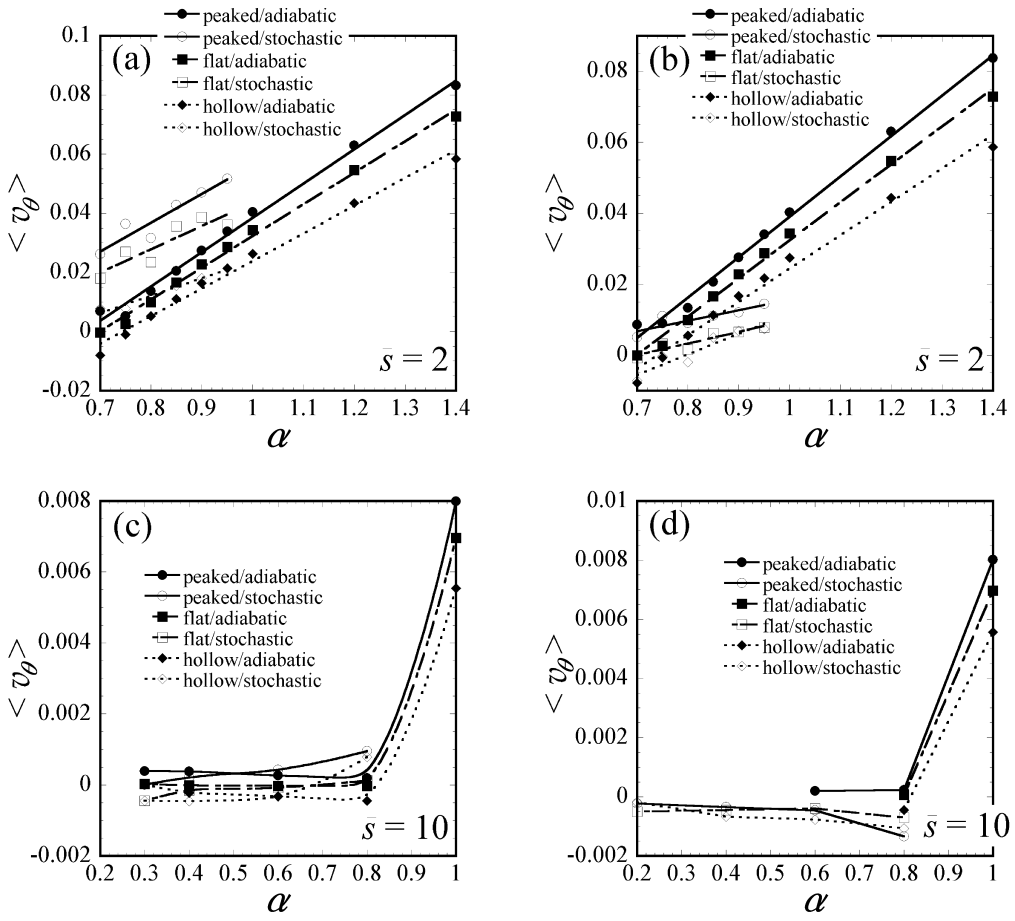

Fig. 4 The azimuthal drift velocity of ions vs. the normalized canonical angular momentum α (a) $\bar{s} = 2$ and elliptic FRC, (b) $\bar{s} = 2$ and racetrack FRC, (c) $\bar{s} = 10$ and elliptic FRC and (d) $\bar{s} = 10$ and racetrack FRC. The lines in Figs. (a) and (b) are drawn linearly with a use of least square method. Although the curves in Fig. (c) are also fitted by the least square, however the lines in (d) are drawn only to guide the reader's eye.

4. Conclusions

Single particle orbits have been traced in the prescribed equilibria inside the separatrix of Field-Reversed Configurations (FRCs). Equilibria with the peaked, flat and hollow current profile have been calculated semi-analytically. The surface of section plot was used for the classification of ion motion, and it is found that the kinetic ions (i.e., fast ions) tend to move adiabatically. Their betatron orbits are never changed, and therefore there is no rapid change of orbit (e.g. from the figure-8 to the small-gyroradius orbit, and vice versa) as a source of randomization process. No azimuthal drift velocity has been found for the slower ions, although they move in non-uniform magnetic field. This suggests that the averaged azimuthal motion due to the diamagnetic curvature drift near the curved magnetic field region is almost the same as the azimuthal motion by the paramagnetic grad-B drift in the neighborhood of midplane. It is found that the stochastic fast ions in the elliptic FRC have a larger drift velocity due to the curvature of the magnetic field. A self-consistent study for the tilt mode stability of FRC with using a hybrid or particle scheme is the subject in a near future.

References

[1] E.V. Belova, S.C. Jardin, H. Ji, M. Yamada and R. Kulsrud, Phys. Plasmas **7**, 4996 (2000).
[2] N. Iwasawa, A. Ishida and L.C. Steinhauer, Phys. Plasmas **7**, 931 (2000).
[3] Y.A. Omelchenko, M.J. Schaffer and P.B. Parks, Phys. Plasmas **8**, 4463 (2001).
[4] D.C. Barnes, Phys. Plasmas **10**, 1636 (2003).
[5] H. Ohtani, R. Horiuchi and T. Sato, Phys. Plasmas **10**, 145 (2003).
[6] R. Horiuchi and T. Sato, Phys. Fluids **B 1**, 581 (1989).
[7] R.D. Milroy, D.C. Barnes, R.C. Bishop and R.B. Webster, Phys. Fluids **B 1**, 1225 (1989).
[8] M. Tuszewski, Nucl. Fusion **28**, 2033 (1988).
[9] Y. Hayakawa, T. Takahashi and Y. Kondoh, Nucl. Fusion **42**, 1075 (2002).
[10] M.J. Hill, Philos. Trans. R. Soc. London, Ser. A **C/XXXV**, 213 (1894).
[11] R. Kanno, A. Ishida and L.C. Steinhauer, J. Phys. Soc. Jpn. **64**, 463 (1995).
[12] N. Iwasawa, Ph. D. thesis, Niigata University 2000.
[13] C. Störmer, *The Polar Aurora* (Oxford University Press, 1955).